Supplementary Material

Behavioural response study on seismic airgun and vessel exposures in narwhals

M.P. Heide-Jørgensen, S.B. Blackwell, O.M. Tervo, A.L. Samson, E. Garde, R.G. Hansen, M.C. Ngô, A.S. Conrad, P. Trinhammer, H.C. Schmidt, M.-H.S. Sinding, T.M. Williams, S. Ditlevsen

A. Number of FastlocGPS positions acquired from whales in different exposure and context situations

The number and temporal resolution of positions may affect the measurements of the horizontal speed of the whales, because more positions may show faster speeds and because positions that are separated further in time may include more curved travel routes of the whales. The effect of difference in time of subsequent positions on speed was tested by linear regression after rejection of outliners, i.e., speed =0 or speed >10 m/s (n=267) and difference in time between positions >1800s (n=1079). This was done on the entire set of speed observations (n=14787, Fig. S1) and on the speed observations from whales that were in trial, intertrial and in pre- and post-trial/-intertrial situations.

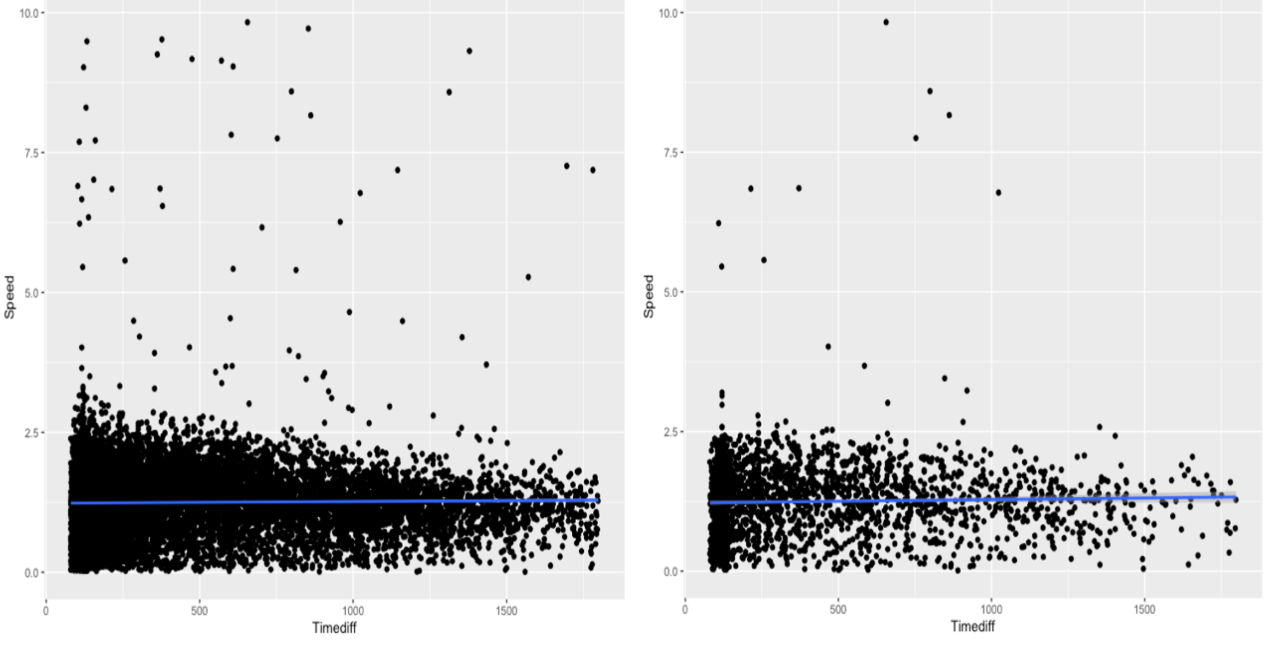

Fig. S1. The relation between horizontal speed of the whales for different time periods between positions. Left shows all data (n=14787), and right shows data from trial, intertrial and pre- and post-trial/intertrial situations (n=2251).

The lack of correlation (r^2=0.0) indicates that the estimated speed of the whales was not influenced by the frequency and spacing in time of the acquired FastlocGPS positions.

The distribution of time between positions for the different contexts before, during and after exposures is shown in Fig. S2.

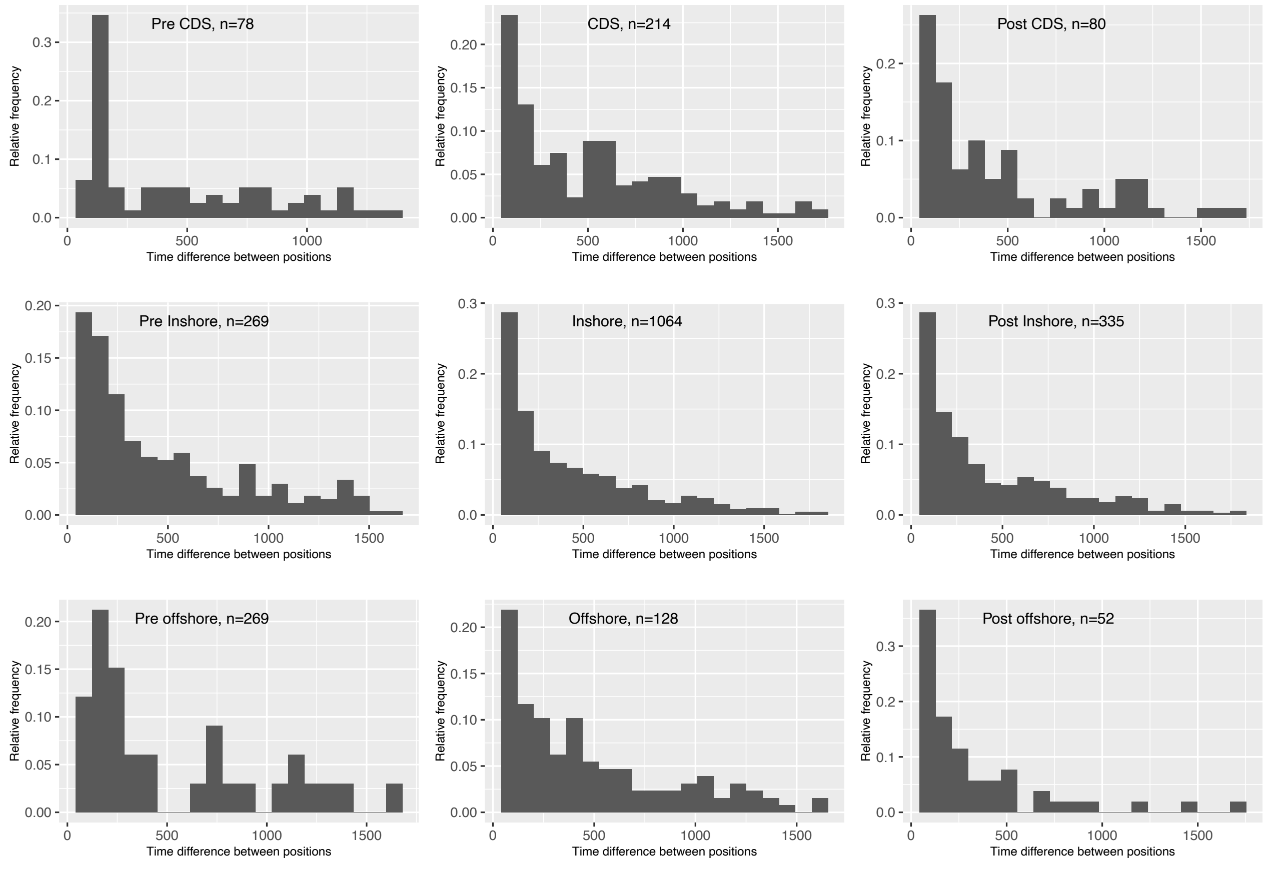

Fig. S2. Histogram of the difference in time between positions for the three different contexts and for periods before, during, and after exposure. CDS = cul de sac.

A Kruskal-Wallis rank sum test did not reveal any significant differences between the frequency distributions of the time between positions (chi-squared = 11.158, df = 8, p-value = 0.1929, figure S3) as also confirmed with a multiple pairwise comparison test (Conover-Iman test with Bonferroni adjustment).

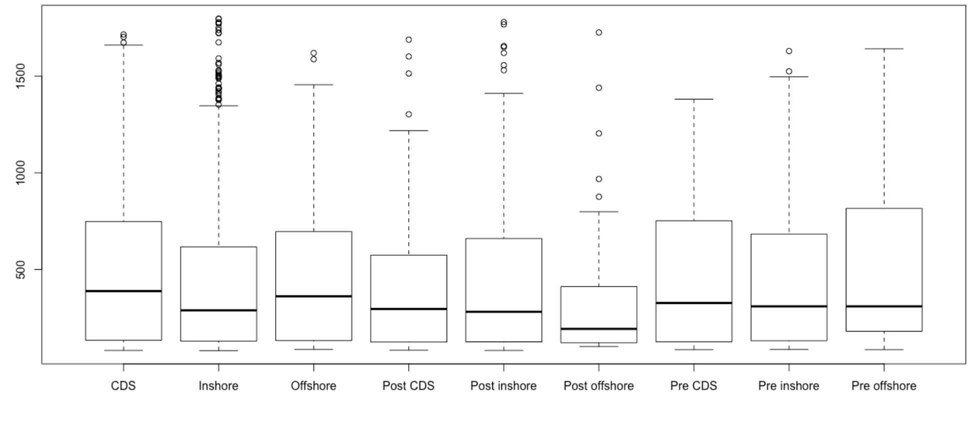

Fig. S3. Box plot of the distributions of difference in timing of positions for the nine context situations. The graph represents the minimum, maximum, median, first and third quartile in the data.

B. Analysis of airgun pulses from SoundTraps and Acousondes

During airgun pulse analyses, pulses with a signal-to-noise ratio (SNR) below 10 dB are generally removed (e.g., Madsen et al. 2006). In light of the unexpectedly low received levels of airgun pulses in this study and the small range over which they were above background noise levels, we used different criteria to increase our sample size. Figure S4 shows analyzed airgun pulses with SNRs above 10 dB (black symbols) and below 10 dB (red symbols). The percentage of analyzed airgun pulses with SNRs above 10 dB was 89% for the large airgun (1040 in^3 or 17.0 liters) and 79% for the small airgun (210 in^3 or 3.45 liters).

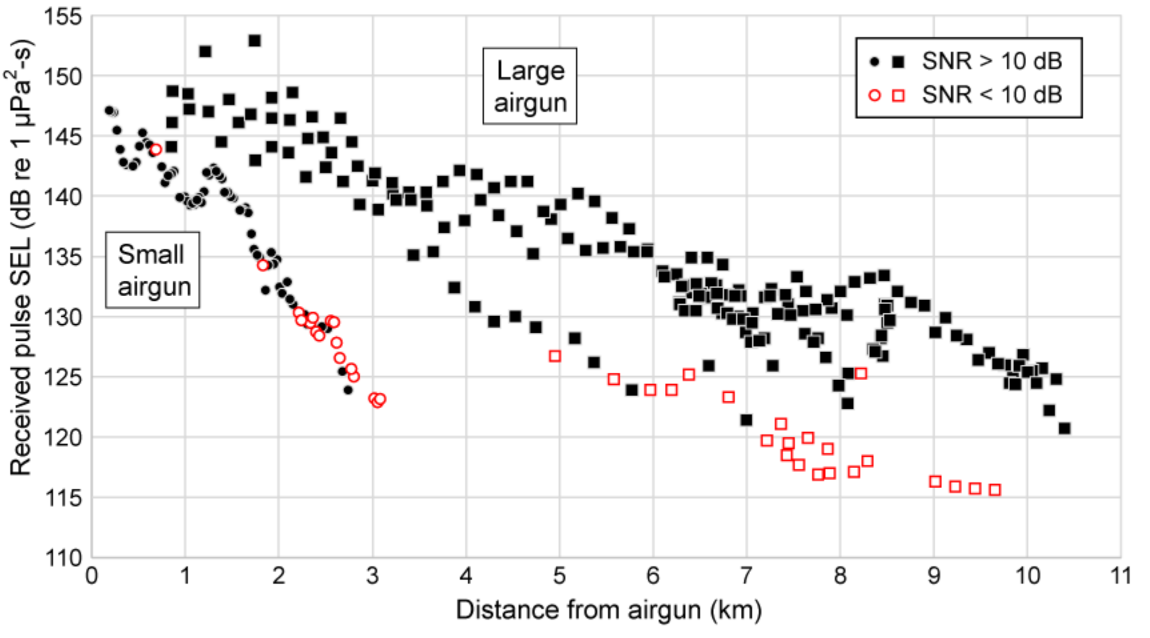

Fig. S4. Received levels of airgun sound (10 Hz–10 kHz) as a function of range, showing whether the SNR was above 10 dB (black symbols) or below 10 dB (red symbols). See the upper part of Fig. 5A in the main body of the paper.

The arrival time of an airgun pulse at the SoundTrap recorder (ST) was calculated based on the shot time and the distance separating the airgun from the ST. Airgun pulses were then analyzed using the 90% energy approach (McCauley et al. 2000, Madsen et al. 2006, Southall et al. 2007). The total energy received during the pulse was first calculated as the time-integral of the instantaneous sound pressure squared, while subtracting background noise. Two examples (blue lines) are shown in figure S5 and S6. The start of the pulse was defined as the time when the 5th percentile of the energy was received (green line), and the end of the pulse as the time when the 95th percentile of the energy was received (red line)—resulting in the pulse including the middle 90% of the pulse energy. The sound exposure level (SEL) of the pulse is the energy received during this period (in dB re 1 μPa^2-s), while the SPL of the pulse (in dB re 1 μPa) is the SEL divided by the duration.

Cumulative sound exposure plots like those shown in figures S5 and S6 were inspected for all analyzed airgun pulses. In these plots, the large, sudden increase in cumulative sound exposure matches the arrival of the pulse. The sound exposure line then flattens out as background levels return to normal.

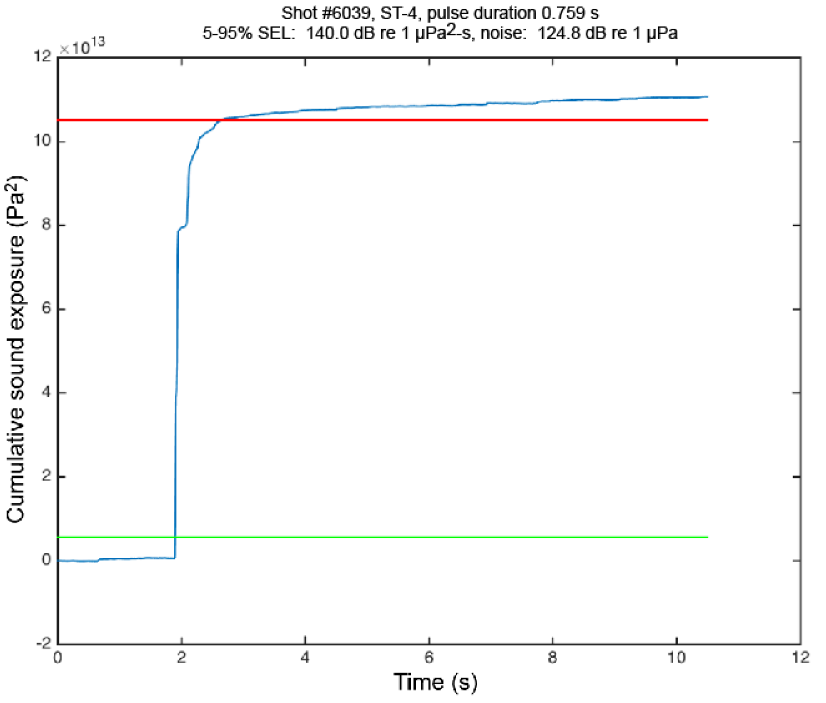

Fig. S5. Cumulative sound exposure plot of excellent quality, with a SNR of 15.2 dB.

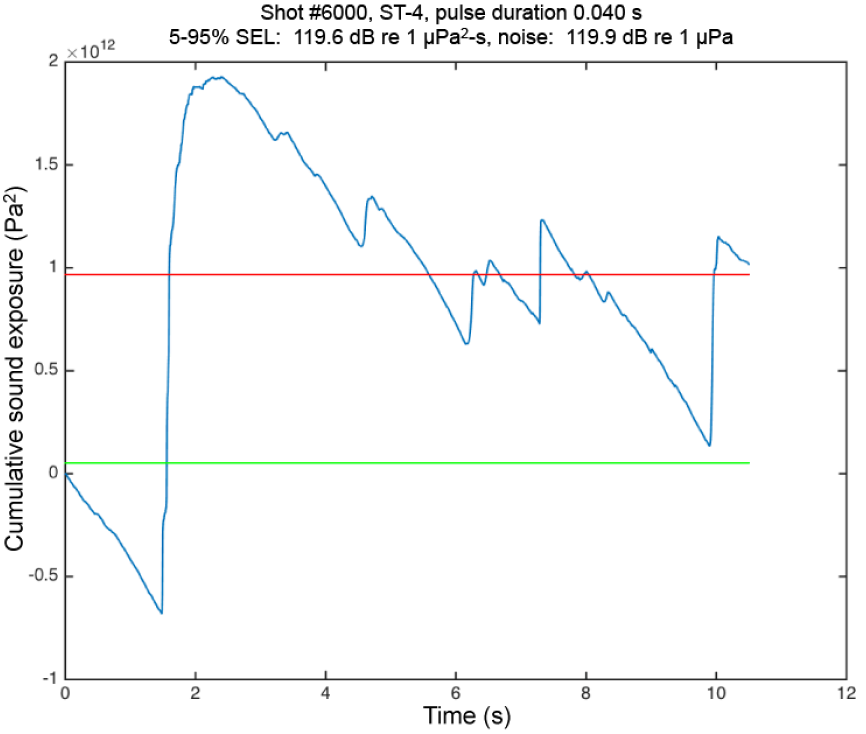

Fig. S6. Cumulative sound exposure plot of poor quality, which was rejected in the analysis. In this particular case, the background was variable and noisy, due to proximity to a glacier with meltwater runoff. The noise level, calculated based on a sample 3 s before the pulse, was too large, as indicated by the downward-sloping baseline (as read from left to right) throughout the plot. The resulting calculated levels are unusable.

Analyzed airgun pulses were discarded for any of the following reasons:

- The largest vertical increase in cumulative sound exposure did not match the expected airgun pulse arrival time or was obviously from some other, non-airgun source.
- The near-horizontal part of the sound exposure line, i.e., preceding and following the arrival of the airgun pulse, indicated that the noise sample was not representative of the average background, being either too large (as in Fig. S6) or too small.

- The pulse duration was unreasonably short (e.g., a few ms) or too long (several seconds); we used the duration of good pulses as a comparative standard.

It should be noted that **pulse durations** were generally longer and more variable (particularly for SNRs below 10 dB) than one might expect, due to reverberation in the fjord environment, and variable, particularly for SNRs below 10 dB. Mean pulse durations (± one S.D.) for the pulses presented in Fig. 5 in the main text were as follows for the four SSVs:

Fønfjord (F), large air gun: 1.6 s ± 0.7 s
Outer Gåsefjord (OG1), large airgun: 1.3 s ± 0.3 s
Outer Gåsefjord (OG2), large airgun: 1.2 s ± 0.9 s
Outer Gåsefjord (OG3), small airgun: 0.7 s ± 0.2 s

Logarithmic fits were used on received airgun pulse SELs (Fig. 5A), but linear fits gave higher r-values. Both types of equations are given below. RL is the received level, x is the range in km.
Small airgun: linear fit $RL = 148.9 - 0.008x$, $r = 0.961$, log fit $RL = 194.9 - 18.7\mathrm{LOG}(x)$, $r = 0.858$
Large airgun: linear fit $RL = 149.3 - 0.003x$, $r = 0.845$, log fit $RL = 235.3 - 27.5\mathrm{LOG}(x)$, $r = 0.838$

Airgun pulses on the Acousonde records were analyzed using the same techniques as described above. In addition to the generally low received levels in the Scoresby Sound environment and the frequency overlap between airgun pulses and flow noise (see Madsen et al. 2006), the tag data included an additional difficulty, which was the high level of flow noise (boundary-layer flow over the Acousonde) on the stroking whales. For example, during high stroking, background levels on the Acousonde tags often exceeded 150 dB re 1 µPa (SPL, 1-sec samples) and occasionally 160 dB, with nothing but stroking noise audible to a listener. Meanwhile, unweighted pulse SPLs as high as 160 dB were never obtained during any of the SSVs and as a result, the majority of the analyzed airgun pulses had received levels near background.

C. Frequency content of airgun pulses

In unweighted data, the pulses were analyzed over the frequency range of 10 Hz–10 kHz, allowing comparisons between airgun pulses received at the SoundTraps and Acousondes to be made (Fig. S7). In analyzed airgun pulses from unweighted data, the contribution of the 10–47 kHz frequency range was very small (<0.001 dB). In the HF-weighted data (as per Southall et al. 2019) from the SoundTraps, analyses were made over the full frequency range of 10 Hz–48 kHz.

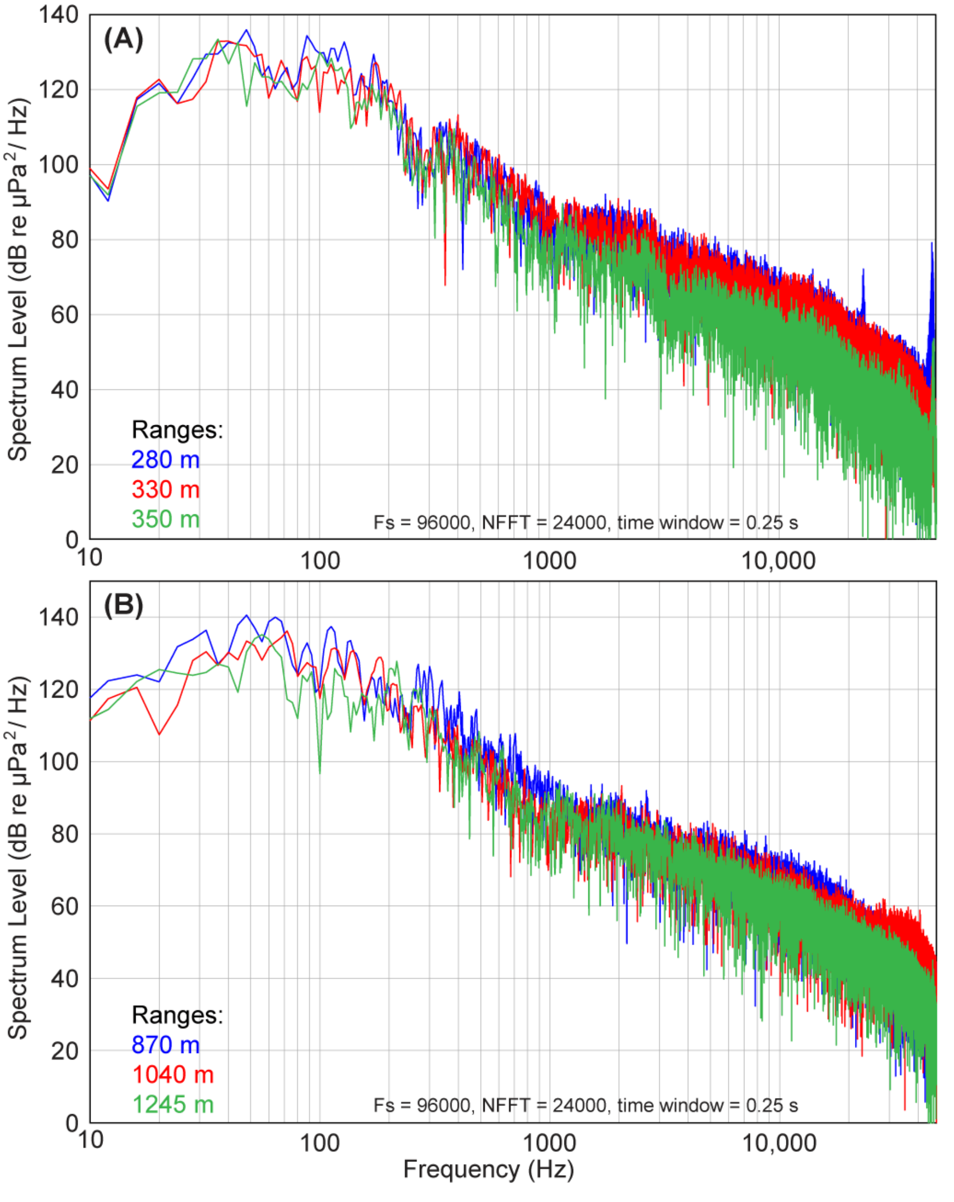

Fig. S7. Spectral plots of airgun pulses. **(A)** Three pulses produced by the small airgun (210 in^3), 31 Aug. 2018 18:36–18:37 GMT, depth 10 m, range 280–350 m. At the 280 m range (blue line), note the presence of the two high-frequency peaks from the MBES (see section D Fig. S8). **(B)** Three pulses produced by the large airgun (1040 in^3), 31 Aug. 2018 8:47–8:50 GMT, depth 10 m, range 870–1245 m.

D. Frequency content of pulses from multi-beam echo sounder (MBES), Reson Seabat 7160

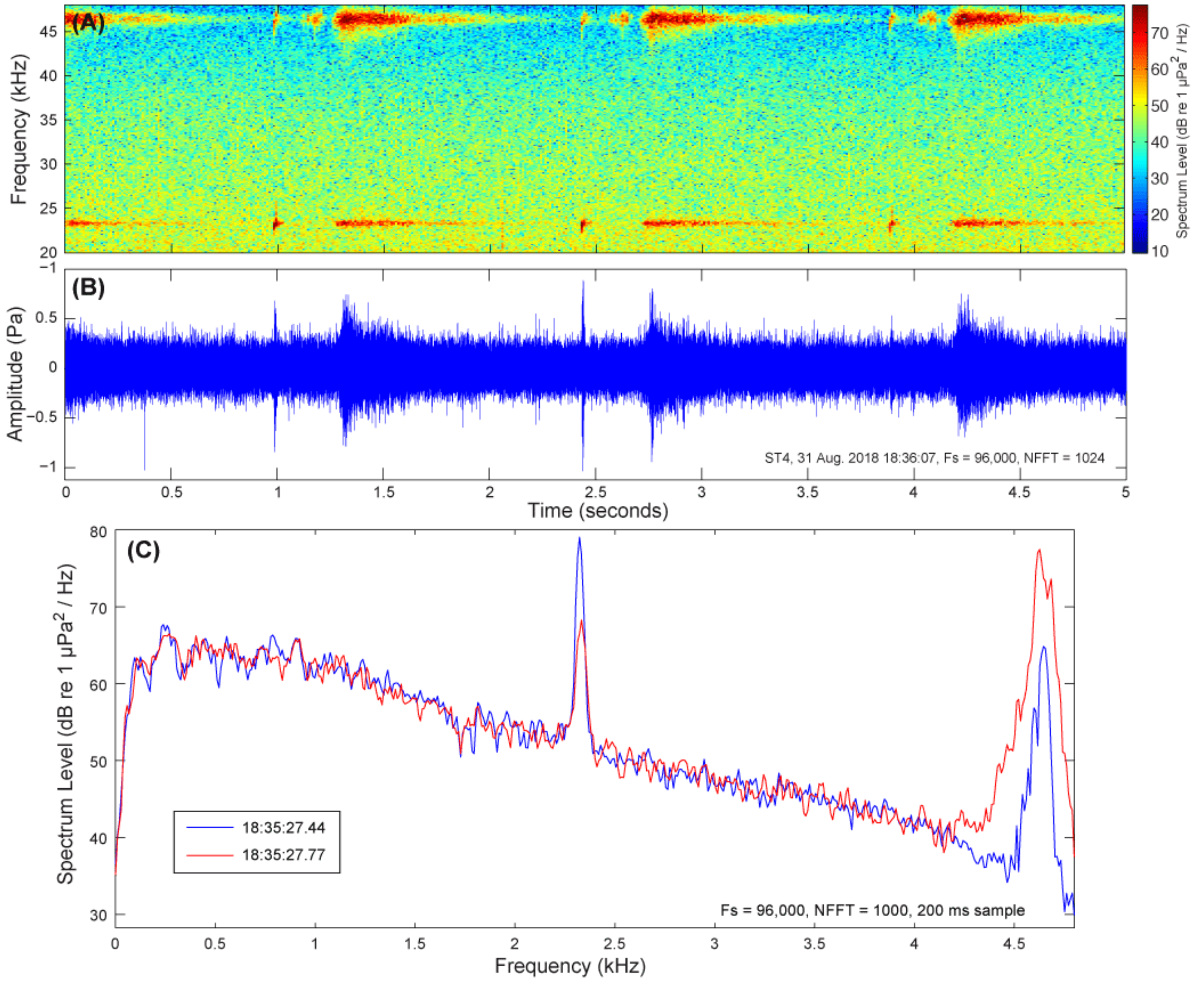

Fig. S8. Spectral composition of the multi-beam echo-sounder (MBES), as shown in HF-weighted data. All samples are from a SoundTrap at 10 m depth on 31 Aug. 2018. ***(A)*** Spectrogram and ***(B)*** sound pressure time series of a 5-s sample obtained 280 m from the vessel (*Lauge Koch*). ***(C)*** Spectrum levels of two 200-ms samples taken 0.33 s apart at a range of 235 m, centered on the two strongest arrivals of the pulse. The first arrival (blue line) is very short (on the order of 30 ms) with a peak near 23 kHz and the second arrival (red line) is longer (>0.5 s), has a wider bandwidth, and a peak near 47 kHz.

E. Mixed effect model of horizontal speed of the whales during exposure in different context

Linearity of residuals, constant variance assumption and normality of residuals were tested with diagnostic plots (Fig. S9).

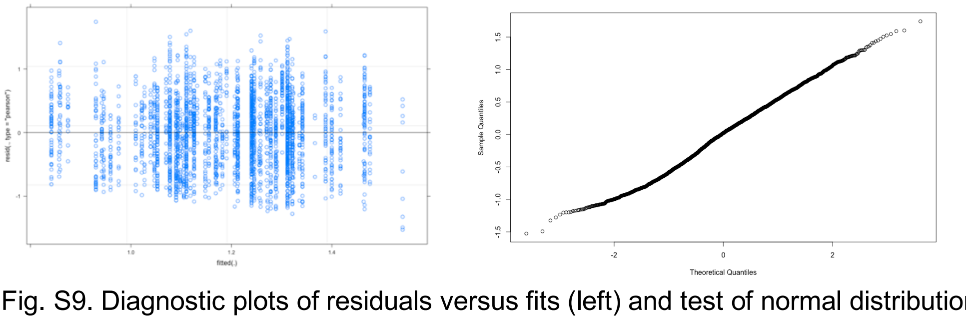

Fig. S9. Diagnostic plots of residuals versus fits (left) and test of normal distribution with q-q plots (right).

Table S1. Pearson correlation coefficients of distance to shore for pairs of whales when simultaneously exposed during intertrials and trials.

	A1	A2	A3	B1	B2	B3	B4	B5	B6
A1	1								
A2	0.82	1							
A3	0.89	0.84	1						
B1	NA	NA	NA	1					
B2	NA	NA	NA	0.94*)	1				
B3	NA	NA	NA	NA	0.38	1			
B4	NA	NA	NA	0.46	0.60**)	0.97***)	1		
B5	NA	NA	NA	0.20	-0.37	-0.96	0.42	1	
B6	NA	NA	NA	-0.30	0.05	0.19	-0.11	0.14	1

*) The two whales were only together for 5 hrs
**) The two whales were only together for 4.5 hrs
***) The two whales were only together for 2 min

Table S2. Summary statistics for the mixed effect model of the horizontal speed of whale groups for pre-exposure during intertrial (reference group) and trial, and for three different context situations (cul-de-sac, inshore and offshore). Estimates with 95% confidence intervals and p-values are provided. The residual variance contribution (σ^2), the contribution from the individual whale (τ), the relative contribution from the whales (ICC), the number of whales involved (N) and the number of observations are shown.

	Speed all			**Speed CDS**			**Speed Inshore**			**Speed offshore**		
Predictors	*Estimates*	*CI*	*p*	*Estimates*	*CI*	*p*	*Estimates*	*CI*	*p*	*Estimates*	*CI*	*p*
(Intercept)	0.90	0.83 – 0.98	**<0.001**	0.87	0.65 – 1.10	**<0.001**	0.81	0.58-1.05	**<0.001**	1.23	0.87-1.59	**<0.001**
Trial	0.30	0.22 – 0.38	**<0.001**	0.39	0.28 – 0.51	**<0.001**	0.33	0.10-0.56	**0.004**	-0.22	-0.41- -0.03	**0.022**
Random Effects												
σ^2	0.26			0.20			0.28			0.19		
τ_{00}	0.00 GROUP			0.06 GROUP			0.01 GROUP			0.18 GROUP		
ICC	0.01			0.22			0.05			0.49		
N	7 GROUP			5 GROUP			6 GROUP			6 GROUP		
Observations	653			300			198			155		

Tabel S3. Speed of the group of whales in four exposure contexts in 2017 (ANOVA).

Intertrial-CDS	*df*	*Sum sq*	*Mean sq*	*F value*	*Pr(>F)*
Context	2	15.44	7.722	31.73	2.76e-13 ***
Residuals	316	76.89	0.243		
	Mean	*CI 95%*			
Pre-intertrial cul-de-sac	0.90	0.81-1.00			
Intertrial cul-de-sac	1.18	1.11-1.26			
Post-intertrial cul-de-sac	1.58	1.43-1.72			
Trial-CDS	*df*	*Sum sq*	*Mean sq*	*F value*	*Pr(>F)*
Context	2	6.16	3.0806	9.992	5.72e-05 ***
Residuals	432	133.18	0.3083		
	Mean	*CI 95%*			
Pre-trial CDS	1.27	1.19-1.35			
Trial CDS	0.99	0.90-1.08			
Post-trial CDS	1.17	1.07-1.26			
Intertrial-Offshore	*df*	*Sum sq*	*Mean sq*	*F value*	*Pr(>F)*
Context	1	4.39	4.387	16.02	8.51e-05 ***
Residuals	224	61.33	0.274		
	Mean	*CI 95%*			
Pre-intertrial offshore	1.53	1.25-1.81			
Intertrial offshore	1.07	1.00-1.14			
Trial-Offshore	*df*	*Sum sq*	*Mean sq*	*F value*	*Pr(>F)*
Context	2	0.586	0.2929	1.804	0.168
Residuals	151	24.518	0.1624		
	Mean	*CI 95%*			
Pre-trial offshore	1.00	0.90-1.10			
Trial offshore	1.14	1.02-1.25			
Post-trial offshore	1.03	0.91-1.15			

Table S4. Summary statistics for the mixed effect model of the horizontal speed in relation to the context of the whales for the exposure study in 2018 with the vessel *Lauge Koch*. Three context situations (cul-de-sac, inshore and offshore) were tested for intertrial (ship only) and trial (ship with airgun) exposures. Estimates with 95% confidence intervals and p-values are provided. The residual variance contribution (σ^2), the contribution from the individual whale (τ), the relative contribution from the whales (ICC), the number of whales involved (N) and the number of observations are shown. The reference group is the pre-exposure (intercept).

Intertrial/trial		**Intertrial cul-de-sac**			**Trial cul-de-sac**			**Intertrial inshore**			**Trial inshore**			**Intertrial offshore**			**Trial offshore**	
Predictors	*Estimates*	*CI*	*p*	*Estimates*	*CI*	*p*	*Estimates*	*CI*	*p*	*Estimates*	*CI*	*p*	*Estimates*	*CI*	*p*	*Estimates*	*CI*	*p*
(Intercept)	0.83	0.69 – 0.97	**<0.001**	1.01	0.56 – 1.46	**<0.001**	0.83	0.57 – 1.09	**<0.001**	1.17	1.03 – 1.31	**<0.001**	0.89	0.64 – 1.14	**<0.001**	1.38	0.96 – 1.79	**<0.001**
Exposure	0.23	0.08 – 0.38	**0.002**	-0.25	-0.47 – -0.03	**0.024**	0.52	0.23 – 0.80	**<0.001**	0.13	0.04 – 0.22	**0.005**	0.49	0.34 – 0.65	**<0.001**	0.08	-0.07 – 0.23	0.288
Post	0.67	0.47 – 0.87	**<0.001**	-0.14	-0.38 – 0.10	0.260	0.58	0.27 – 0.90	**<0.001**	0.23	0.11 – 0.34	**<0.001**	0.34	0.19 – 0.49	**<0.001**	-0.14	-0.32 – 0.03	0.111
Random Effects																		
σ^2		0.29			0.15			0.34			0.29			0.19			0.15	
τ		0.00 WHALE			0.16 WHALE			0.00 WHALE			0.02 WHALE			0.06 WHALE			0.12 WHALE	
ICC		0.02			0.52						0.07			0.24			0.45	
N		4 WHALE			4 WHALE			3 WHALE			6 WHALE			5 WHALE			3 WHALE	
Observations		272			135			152			1008			275			205	

F. Threshold values for distance to shore

Table S6. Percentage time spent close to the coast with different thresholds for nine whales exposed to seismic in 2017 (A1-A3) and 2018 (B1-B6).

Whale	Distance thresholds		
	235 m	200 m	150 m
A1	3.7 %	2.6 %	0.6 %
A2	1.1 %	0.9 %	0.3 %
A3	4.3 %	2.7 %	1.0 %
B1	40.4 %	25.3 %	19.1 %
B2	26.0 %	17.5 %	11.0 %
B3	62.0 %	36.0 %	32.3 %
B4	26.5 %	19.7 %	15.6 %
B5	7.6 %	4.5 %	2.5 %
B6	17.8 %	14.0 %	11.6 %

G. Example of video-clip of whale track

Video clip S1. Whale (B4) tracked in 2018 (blue dot) with Acousonde (red diamond) that was on the whale until 2018-08-29 12:23:37. The seismic vessel *Lauge Koch* is shown with a green triangle and when the airgun is active a green diamond is shown. The black dots indicate deployment of Sound Trap recorders. The red heart in the beginning of the track indicates that the whale was also instrumented with a heart-rate recorder that came off shortly after the whale was released.

References

Madsen, P.T., Johnson, M., Miller, P.J.O., Lynch, J., and Tyack, P. (2006). Quantitative measures of air-gun pulses recorded on sperm whales (*Physeter macrocephalus*) using acoustic tags during controlled exposure experiments. *J. Acoust. Soc. Am.* 120, 2366–2379.

McCauley, R.D., Fewtrell, J., Duncan, A.J., Jenner, C., Jenner, M.-N., and Penrose, J.D., et al. (2000). Marine seismic surveys—A study of environmental implications, APPEA (Australian Petroleum Production and Exploration Association) J. 40, 692–708.

Southall, B. L., Bowles, A. E., Ellison, W. T., Finneran, J. J., Gentry, R. L., Greene, C. R., et al. (2007). Marine mammal noise exposure criteria: Initial scientific recommendations. *Aquat. Mamm.* 33, 411–521.

Southall, B.L., Finneran, J.J., Reichmuth, C., Nachtigall, P.E., Ketten, D.R., Bowles, A.E., et al. (2019). Marine mammal noise exposure criteria: updated scientific recommendations for residual hearing effects. *Aquat. Mamm*. 45, 125–232.